THERMAL RADIATION EFFECTS ON MHD UNSTEADY COUETTE FLOW HEAT AND MASS TRANSFER FREE CONVECTIVE IN VERTICAL CHANNELS DUE TO RAMPED AND ISOTHERMAL TEMPERATURE

F. Abdullahi, M.A Sani, D.A. Sani, M.M. Sani, M. Ibrahim, F. Abubakar and I.M. Garba

Department of Mathematics
Waziri Umaru Federal Polytechnic
Birnin Kebbi, Kebbi State
Email: farukabdullahi@wufpbk.edu.ng

Abstract
Numerical investigations were carried out to study thermal radiation effects on magneto-hydrodynamics (MHD) unsteady Couette flow heat mass transfer free-convective in vertical channels due to ramped and isothermal temperature. The governing coupled non-linear partial differential equations of the flow were transformed into non-dimensional form using suitable dimensional quantities. Finite element method (FEM) was employed to find numerical solution of the dimensionless governing coupled boundary layer partial differential equations. The expressions of velocity, temperature, concentration, skin friction, Nusselt number as well as Sherwood number have been obtained and discussed using line graph. From the outcome of the result it was revealed that, increase of porosity parameter K, ratio of mass transfer parameter N, Time parameter t, Eckert number Ec enhances the velocity and temperature while reverse is the case with the with increase of Magnetic parameter M, Radiation parameter tern R and Prandtl number $\Pr$. At y = 0, the fluid skin friction gets enlarged with increase in porosity parameter K, Nusselt number gets increased with increase of Prandtl number $\Pr$ and Sherwood number gets boosted with increase of Eckert number Ec. Similarly, at y = 1 skin friction gets enhanced with increase of porosity parameter K, Nusselt number diminishes with increase of Prandtl number $\Pr$ and Sherwood number gets enlarged with increase of Eckert number Ec.

Keywords: *MHD, thermal radiation effects, isothermal temperature, ramped temperature*

1. Introduction

Studying thermal radiation effects on magneto-hydrodynamics (MHD) has attracted the interest of many researchers in applied mathematics and engineering sciences due to the applications of such flows in the context of aerodynamics. The process by which energy is emitted from one body to another as electromagnetic waves or as moving subatomic particles is known as radiation. Emission of electromagnetic energy results in a decrease in the energy level which is vital in temperature stabilization. Heat transfer problems are classified according to the variable that the temperature depends upon. For example if the temperature is independent of time, the problem is referred to steady-state problem, while on the other hand if the temperature is a function of time, the problem is classified as unsteady or transient.

The study of MHD flow has attracted a lot of attentions from many researchers as a result of its wide applications in astrophysics and geophysics. It is applied to the study of stellar and solar structures, interstellar matter, and radio propagation through the ionosphere. In engineering, it is applied in MHD pumps, MHD bearings, nuclear reactors, geothermal energy extraction and in boundary layer control in the field of aerodynamics. Animasaun, Raju and Sandeep (2016) analyzed effects of nonlinear thermal radiation and induced magnetic field on viscoelastic fluid flow toward a stagnation point. Similarly Bala, Kumar and Lin (2016) studied the nonlinear coupled evolution equations, which modeled the transient MHD natural convection and mass transfer flow of viscous, incompressible and electrically conducting fluid between two infinite vertical plates. This study was carried out in the presence of the transversal magnetic field, thermal radiation, thermal diffusion and diffusion-thermo effects. They discovered that as the radiation, temperature difference, sustention parameter, thermal-diffusion, diffusion-thermo, and non-dimensional time parameters increase, both the velocity and temperature increase. Furthermore, Ganesh, Gireesha, Manjunatha and Rudraswamy (2017) analyzed the effect of nonlinear thermal radiation on double diffusive free convective boundary layer flow of a viscoelastic nanofluid over a stretching sheet. They discovered increasing values of temperature ratio parameter θ_w extinguishes the rate of heat transfer $|\theta'(0)|$ for fixed Pr and R, also the temperature ratio parameter θ_w and the thermal radiation parameter R have the same effect.

Bhatti, Zeeshan, and Ellahi (2017) studied the effects of heat transfer on particle fluid suspension induced by metachronal. Their study revealed that an increment in thermal radiation R and Casson fluid parameter Δ causes a reduction in the temperature profile when the influence of MHD and thermal radiation are taken into consideration through the help of Ohm’s law and Roseland’s approximation. Additionally, Ganesh et al. (2017) analyzed two-phase boundary layer flow and heat transfer of a Williamson fluid with fluid particle suspension over a stretching sheet. The region of temperature jump and nonlinear thermal radiation was considered in the energy transfer process. They reported that, the thermal boundary layer thickness gets thinner due to increase in temperature jump parameter. They also revealed that intensifying of β_v and β_t reduces fluid phase velocity and temperature profile. Alao, Fagbade and Falodun (2016) studied the influence of some thermo-physical properties of fluid on heat and mass transfer flow past semi-infinite moving vertical plate. The fluid considered was optically thin in such a way that the thermal heat loss on the fluid is modeled using Rosseland approximation. They revealed that an increase in the thermal radiation parameter leads to the boosting of both the velocity and temperature profiles. They further revealed that the velocity profile as well as the concentration profile gets enhanced with an increase in the Soret number.

In the study of Shagaiya and Simon (2015) the influence of buoyancy and thermal radiation on MHD flow over a stretching porous sheet was analyzed. Their model which highly constituted nonlinear governing equations was transformed using similarity solution and then solved using homotopy analysis method (HAM). From their research it was found that when the buoyancy parameter increases, the fluid velocity gets enlarged and the thermal boundary layer gets reduced. In case of the thermal radiation, they observed that increasing the thermal radiation parameter produces significant enhancement in the thermal conditions of the fluid temperature. This causes more fluid in the boundary layer due to buoyancy effect, causing the velocity in the fluid to increase. The hydrodynamic boundary layer and thermal boundary layer thicknesses were observed to increase as a result of increasing radiation. Nayak (2017) studied three dimensional (MHD) flow and heat transfer analysis associated with thermal radiation as well as viscous dissipation of nanofluid over a shrinking surface. He found that temperature the thermal boundary gets enhanced due to increase in viscous dissipation which leads to thicker thermal boundary layer. He also revealed that enlarging the temperature is simply increasing the radiation parameter, R. He further revealed that there is an increase in fluid velocity when suction is present at the shrinking surface. Moreover, Rizwan, Nadeem, Hayat and Sher (2015) studied the stagnation point flow of nanofluid with MHD and thermal radiation effects passed over a stretching sheet. Moreover, they considered the combined effects of velocity and thermal slip and found that rising in Hartmann number gives the resistive type flow within the boundary layer; consequently velocity profile shows the decreasing behavior with an increase of M. The thermal slip parameter provides the decreasing behavior in the temperature profile. While on the other hand radiations parameters give rise in temperature profile.

Siva and Anjan (2016), studied finite element analysis of heat and mass transfer past an impulsively moving vertical plate with ramped temperature. From their study the velocity gets intensified with increase of the values of thermal buoyancy force, solutal buoyancy force, permeability parameter and time. Shagaiya and Daniel (2015) investigated the theoretical influence of buoyancy and thermal radiation on MHD flow over a stretching porous sheet. He reported that, increasing the thermal radiation parameter produces significant enhancement in the thermal conditions of the fluid temperature which led to more fluid in the boundary layer due to buoyancy effect, causing the velocity in the fluid to increase. From the analysis of Adamu and Bandari (2018) the thermal and solutal buoyancy parameters on the nanofluid flow, heat, and mass transfer characteristics due to a stretching sheet in the presence of a magnetic field were studied. They discovered that, the axial velocity of the fluid get increased with an increase of both thermal and solutal buoyancy parameter, while the thermal conductivity of the fluid get reduced. In the research of Danjuma, Haliru, Ibrahim and Hamza (2019), the influence of unsteady Heat Transfer to MHD Oscillatory flow of Jeffrey fluid through a porous medium under slip condition analyzed. They reported that, the temperature profile gets enhanced with increasing Peclet number and the velocity profile gets reduced with increasing Hartmann number and Dacy number. Reddy, Raju and Rao and Gola (2017) analyzed the influence of an unsteady magneto-hydrodynamics natural convection on the Couette flow of electrically conducting water at 4^0 C (Pr = 11.40) in a rotating system. The primary velocity, secondary velocity and temperature of water at 4^o C as well as shear stresses and rate of heat transfer were obtained for both ramped temperature and isothermal plates.

The present numerical investigation analyzed finite element analysis of thermal radiation effects on unsteady MHD heat mass transfer Couette flow in free convective vertical channels due to ramped and isothermal temperature. The governing coupled, non-linear, partial differential equations of the flow were solved using finite element method. The velocity, temperature, concentration as well as shear stress have been obtained for both and continuous ramped temperature isothermal plates.

2. Formulation of the Problem

Consider an unsteady free convection flow of an incompressible electrically conducting viscous dissipative fluid past an infinite vertical porous plate. Let the x* -axis be chosen along the plate in the vertically upward direction and the y* axis is chosen normal to the plate. A uniform magnetic field of intensity H_0 is applied transversely to the plate. The induced magnetic field is neglected as the magnetic Reynolds number of the flow is taken to be very small. Initially, the temperature of the plate T^* and the fluid T_w^* are assumed to be the same. The concentration of species at the plate C_w^* and C_0^* are assumed to be the same. At time t*>0, the plate temperature is changed to T_w^*, which is then maintained constant, causing convection currents to flow near the plate and mass is supplied at a constant rate to the plate. Under these conditions the flow variables are functions of time y* and t* alone. The problem is governed by the following equations:

$$\frac{\partial u^*}{\partial t^*} = \frac{\partial^2 u^*}{\partial y^{*2}} + g\beta^{\bullet}(C^* - C_0) - \frac{\sigma \mu_e{}^2 H_0{}^2 u^*}{\rho} - \frac{\nu u^*}{K^*} \tag{1}$$

$$\rho C_p \frac{\partial T^*}{\partial t^*} = k\frac{\partial^2 T^*}{\partial y^{*2}} + \mu\left[\frac{\partial u^*}{\partial y^*}\right]^2 - R^*\theta^* \tag{2}$$

$$\frac{\partial C^*}{\partial t^*} = D_M \frac{\partial^2 C^*}{\partial y^{*2}} \tag{3}$$

The corresponding initial and boundary conditions are:

Case I: Isothermal Temperature

$$\left.\begin{array}{l} t^* \le 0,\ u^* = 0,\ T^* = T_0 \ \ for\ \ all\ \ 0 \le y^* \le L \\ t^* > 0 \begin{cases} u^* = u,\ T^* = T_w,\ C^* = C_w^* \ \ at\ \ y^* = 0 \\ u^* = 0, T^* = 0^* T,\ C^* = C_w^* \ \ at\ \ y^* = L \end{cases} \end{array}\right\}$$

Case II: Continuous Ramped Temperature

$$\left.\begin{array}{l} t^* \le 0,\ u^* = 0,\ T^* = T_0 \ \ for\ \ all\ \ 0 \le y^* \le L \\ t^* > 0 \begin{cases} u^* = u,\ T^* = T_0 + \dfrac{(T_w^* - T_0)t^*}{T_R},\ C^* = C_w^* \ \ at\ \ y^* = 0 \\ u^* = 0, T^* = 0T,\ C^* = C_w^* \ \ at\ \ y^* = L \end{cases} \end{array}\right\} \tag{4}$$

We now introduce the following non- dimensional quantities into the basic equations and initial and boundary conditions in order to make them dimensionless

$$\left.\begin{aligned}
&U_0 = (vg\beta\Delta T)^{1/3}, \quad \mathrm{L}=\left(\frac{\mathrm{g}\beta\Delta\mathrm{T}}{\mathrm{v}^2}\right)^{-1/3} \quad \mathrm{T}_R = \frac{(g\beta\Delta T)^{-2/3}}{v^{-1/3}} \\
&\Delta T = T_w^* - T_\infty^*, \quad \mathrm{t}=\frac{\mathrm{t}^*}{\mathrm{T_R}}, \quad \mathrm{y}=\frac{\mathrm{y}^*}{L}, \quad \mathrm{r_t} = \frac{r^*_t - T_0}{T^*_w - T_0} \\
&u = \frac{u^*}{U_0}, \quad \mathrm{K}=\frac{\mathrm{K}^*}{\mathrm{vT_R}}, \quad \theta=\frac{\mathrm{T}^* - T_0}{T_w^* - T_0}, \quad \phi=\frac{\mathrm{C}^* - C_0}{C_w^* - C_0} \\
&\mathrm{Pr} = \frac{\mu C_P}{k}, \quad \mathrm{Sc}=\frac{\mathrm{v}}{\mathrm{D_m}}, \quad Ec = \frac{U_0^2}{C_P\Delta T}, \quad \mathrm{Sr}=\frac{\mathrm{T_w} - T_0}{C_w - C_0} \\
&N = \frac{\beta^\bullet(C_w^* - C_\infty^*)}{\beta(T_W^* - T_\infty^*)}, \quad M = \frac{\sigma\mu_0^2 H_0^2 T_R}{\rho}
\end{aligned}\right] \tag{5}$$

On the substitution of equations (5) into (1) - (4) the following governing equations in non-dimensional form are obtained.

$$\frac{\partial u}{\partial t} = \frac{\partial^2 u}{\partial y^2} + Gr\theta + N\phi - \left(M + \frac{1}{K}\right)u \tag{6}$$

$$Pr\frac{\partial\theta}{\partial t} = \frac{\partial^2\theta}{\partial y^2} + Ec\left(\frac{\partial u}{\partial y}\right)^2 - \theta R \tag{7}$$

$$Sc\frac{\partial\phi}{\partial t} = \frac{\partial^2\phi}{\partial y^2} \tag{8}$$

The corresponding initial and boundary conditions are

Case I: Isothermal Temperature

$$\left.\begin{aligned}
&t \le 0,\ u = 0, \theta = 0, \phi = 0 \ \ for \ \ all \ \ y \\
&For \ \ t \ge 0: \\
&u = 1, \theta = 1, \phi = 1 \qquad at \ \ y = 0 \\
&u = 0, \theta = 0, \phi = 0 \quad at \ \ y = 1
\end{aligned}\right\}$$

Case II: Continuous Ramped Temperature

$$\left.\begin{aligned}
&t \le 0,\ u = 0, \theta = 0, \phi = 0 \ \ for \ \ all \ \ y \\
&For \ \ t \ge 0: \\
&u = 1, \theta = t, \phi = 1 \qquad at \ \ y = 0 \\
&u = 0, \theta = 0, \phi = 0 \quad at \ \ y = 1
\end{aligned}\right\} \tag{9}$$

3. Method of the Solution

Equations (6) – (8) are a coupled non-linear system of partial differential equations and were to be solved under the boundary conditions (9) using highly validated and robust method known as finite element method (Galerkin approach).

By applying Galerkin finite element method for equation (6) over the element ℓ, $y_i \le y \le y_j$ is

$$\int_{y_i}^{y_i}\left\{N^T\left[\frac{\partial^2 u}{\partial y^2}-\frac{\partial u}{\partial t}-u(M+\frac{1}{K})+Nf+q\right]\right\}dy=0 \tag{10}$$

Equation (10) is reduce to:

$$\int_{y_i}^{y_i}\left\{N^T\left[\frac{\partial^2 u}{\partial y^2}-\frac{\partial u}{\partial t}-M_1u+P\right]\right\}dy=0 \tag{11}$$

Where $M_1 = M+\dfrac{1}{K}$ and $P=\theta+N\phi$

Applying integration by part to equation (10) yield:

$$[N^T\frac{\partial u}{\partial t}]_{y_i}^{yj}-\int_{y_i}^{y_i}\frac{\partial N^T}{\partial y}\frac{\partial u}{\partial y}dy-\int_{y_i}^{y_i}N^T\frac{\partial u}{\partial t}dy-M_1\int_{y_i}^{y_i}N^T u dy+P\int_{y_i}^{y_i}N^T dy=0 \tag{12}$$

Dropping the first term of equation (3.18):

$$\int_{y_i}^{y_i}\frac{\partial N^T}{\partial y}\frac{\partial u}{\partial y}dy+\int_{y_i}^{y_i}N^T\frac{\partial u}{\partial t}dy+M_1\int_{y_i}^{y_i}N^T u dy-P\int_{y_i}^{y_i}N^T dy=0 \tag{13}$$

Let $u^{(e)}=u_iN_i+u_jN_j \Rightarrow u^{(e)}=[N][u]^T$ be a linear piecewise approximation solution over the two nodal element $e,\ (y_i\le y\le y_j)$ where $u^{(e)}=[u_i\ u_j]$, $N=[N_iN_j]$ also u_i *and* u_j are the velocity component at the i^{th} and j^{th} nodes of the typical element (e) $(y_i\le y\le y_j)$ furthermore, N_i and N_j are basis (or shape) functions defined as follows:

$$N_i=\frac{y_j-y}{y_j-y_i},\ N_j=\frac{y-y_i}{y_j-y_i}$$

Hence equation (13) after simplifying becomes:

$$\int_{y_i}^{y_i}\begin{bmatrix}N_i'N_i' & N_i'N_j'\\ N_i'N_j' & N_j'N_j'\end{bmatrix}\begin{bmatrix}u_i\\ u_j\end{bmatrix}dy+\int_{y_i}^{y_i}\begin{bmatrix}N_iN_i & N_iN_j\\ N_iN_j & N_jN_j\end{bmatrix}\begin{bmatrix}\dot{u}_i\\ \dot{u}_j\end{bmatrix}dy+M_1\int_{y_i}^{y_i}\begin{bmatrix}N_iN_i & N_iN_j\\ N_iN_j & N_jN_j\end{bmatrix}\begin{bmatrix}u_i\\ u_j\end{bmatrix}dy-P\int_{y_i}^{y_i}\begin{bmatrix}N_i\\ N_j\end{bmatrix}dy=0 \tag{14}$$

Also simplifying equation (14) above we have:

$$\frac{1}{l}\begin{bmatrix} 1 & -1 \\ -1 & 1 \end{bmatrix}\begin{bmatrix} u_i \\ u_j \end{bmatrix} + \frac{l}{6}\begin{bmatrix} 2 & 1 \\ 1 & 2 \end{bmatrix}\begin{bmatrix} \dot{u}_i \\ \dot{u}_j \end{bmatrix} + \frac{M_1 l}{6}\begin{bmatrix} 2 & 1 \\ 1 & 2 \end{bmatrix}\begin{bmatrix} u_i \\ u_j \end{bmatrix} - \frac{lP}{2}\begin{bmatrix} 1 \\ 1 \end{bmatrix} = 0 \tag{15}$$

Where $l = y_j - y_i = h$ and prime and dot denotes differentiation with respect to y and t respectively. Assembling the equations for the two consecutive elements $y_{i-1} \le y \le y_i$ and $\mathrm{y_i} \le y \le y_{i+1}$ the following is obtained:

$$\frac{1}{l^2}\begin{bmatrix} 1 & -1 & 0 \\ -1 & 2 & -1 \\ 0 & -1 & 1 \end{bmatrix}\begin{bmatrix} u_{i-1} \\ u_i \\ u_{i+1} \end{bmatrix} + \frac{1}{6}\begin{bmatrix} 2 & 1 & 0 \\ 1 & 4 & 1 \\ 0 & 1 & 2 \end{bmatrix}\begin{bmatrix} \dot{u}_{i-1} \\ \dot{u}_i \\ \dot{u}_{i+1} \end{bmatrix} + \frac{M}{6}\begin{bmatrix} 2 & 1 & 0 \\ 1 & 4 & 1 \\ 0 & 1 & 2 \end{bmatrix}\begin{bmatrix} u_{i-1} \\ u_i \\ u_{i+1} \end{bmatrix} - \frac{P}{2}\begin{bmatrix} 1 \\ 2 \\ 1 \end{bmatrix} \tag{16}$$

Now if we consider the row corresponding to the node i to zero with $l = h$, from equation (16) the difference schemes reads:

$$\frac{1}{h^2}(-u_{i-1} + 2u_i - u_{i+1}) + \frac{1}{6}(-\dot{u}_{i-1} + 4\dot{u}_i + \dot{u}_{i+1})\frac{M_1}{6}(u_{i-1} + 4u_i + u_{i+1}) = P \tag{17}$$

Using the trapezoidal rule on (17), the following system of equations in Crank-Nicolson method are obtained as:

$$A_1 u_{i-1}^{n+1} + A_2 u_i^{n+1} + A_3 u_{i+1}^{n+1} = A_4 u_{i-1}^{n} + A_5 u_i^{n} + A_6 u_{i+1}^{n} + P^* \tag{18}$$

Similarly, by solving (7) and (8) using the same method we have:

$$B_1 q_{i-1}^{n+1} + B_2 q_i^{n+1} + B_3 q_{i+1}^{n+1} = B_4 q_{i-1}^{n} + B_5 q_i^{n} + B_6 q_{i+1}^{n} + Q^* \tag{19}$$

$$C_1 \phi_{i-1}^{n+1} + C_2 \phi_i^{n+1} + C_3 \phi_{i+1}^{n+1} = C_4 \phi_{i-1}^{n} + C_5 \phi_i^{n} + C_6 \phi_{i+1}^{n} \tag{20}$$

Where:

$$A_1 = 2 - 6r + rM_1h^2, \quad A_2 = 8 + 12r + rM_1h^2, \quad A_3 = 2 - 6r + rM_1h^2$$

$$\mathrm{A}_4 = 2 + 6r - rM_1h^2, \quad A_5 = 8 - 12r - 4rrM_1h^2, \quad A_6 = 2 + 6r - rM_1h^2$$

$$B_1 = Pr - 3r, \quad B_2 = 4Pr + 6r\,, \quad B_3 = \mathrm{Pr} - 3r \quad \mathrm{B}_4 = Pr + 3r,$$

$$\mathrm{B}_5 = 4Pr - 6r, \quad \mathrm{B}_6 = Pr + 3r$$

$$C_1 = Pr - 3r, \qquad C_2 = 4Pr + 6r\ , \qquad C_3 = \mathrm{Pr} - 3r$$

$$\mathrm{C}_4 = Pr + 3r, \qquad \mathrm{C}_5 = 4Pr - 6r, \qquad \mathrm{C}_6 = Pr + 3r$$

$$\mathrm{P}^* = 12rh^2(\theta_i^n + N\phi_i^n), \quad \text{and} \quad \mathrm{Q}^* = 6r\,\mathrm{Pr}\,Ec\left(\left[\frac{\partial u}{\partial y}\right]^2 - R\theta\right)$$

With $r = \frac{k}{h^2}$ and h and k are the mesh size along y direction and time direction respectively. Index i refers to space and j refers to the time. In equations (18), (19) and (20), taking $i = 1(1)n$ and using the initials and boundary conditions (9), the following system of equations is obtained

$$A_i X_i = B_i \qquad i = 1(1)n$$

Where A_i matrices of are order n and X_i and B_i are column matrices having n components. The solution of the system of equation are obtained using Thomas algorithm for velocity, temperature and concentration. For various parameters the results are computed and p resented graphically.

The skin friction, Nusselt number and Sherwood number are important physical parameters for this type boundary layers flow. With known values of velocity, temperature and concentration fields. The skin-friction at the plate is given by non-dimensional form:

$$\tau = \left[\frac{\partial u}{\partial y}\right]_{y=0,1} \tag{21}$$

The rate of heat transfer coefficient can be obtained in the terms of Nusselt number in non-dimensional form as

$$N_u = -\left[\frac{\partial \theta}{\partial y}\right]_{y=0,1} \tag{22}$$

The rate of mass transfer coefficient cab be obtained in terms of Sherwood number in non-dimensional form given by

$$S_h = -\left[\frac{\partial \phi}{\partial y}\right]_{y=0,1} \tag{23}$$

4. Results and Discussion

In order to analyze the effects various parameters on flow field in the boundary layer region, Finite element method was employed to solve equations (6) to (8) under the boundary conditions (9). We studied the effects Prandtl number Pr, Radiation parameter R, Eckert number Ec Schmidt number Sc, magnetic parameter M, porosity parameter K, Buoyancy effect parameter r_t, ratio of mass transformation (N) on fluid velocity, temperature and concentration and they were presented graphically. $\Pr = 0.71, R = 0.5, Ec = 0.1, Sc = 0.5, M = 0.5, K = 0.5\ r_t = 0.5, N = 0.5$. The values above were adopted to be default parameters values under the present study. There velocity profiles are presented in the following figures:

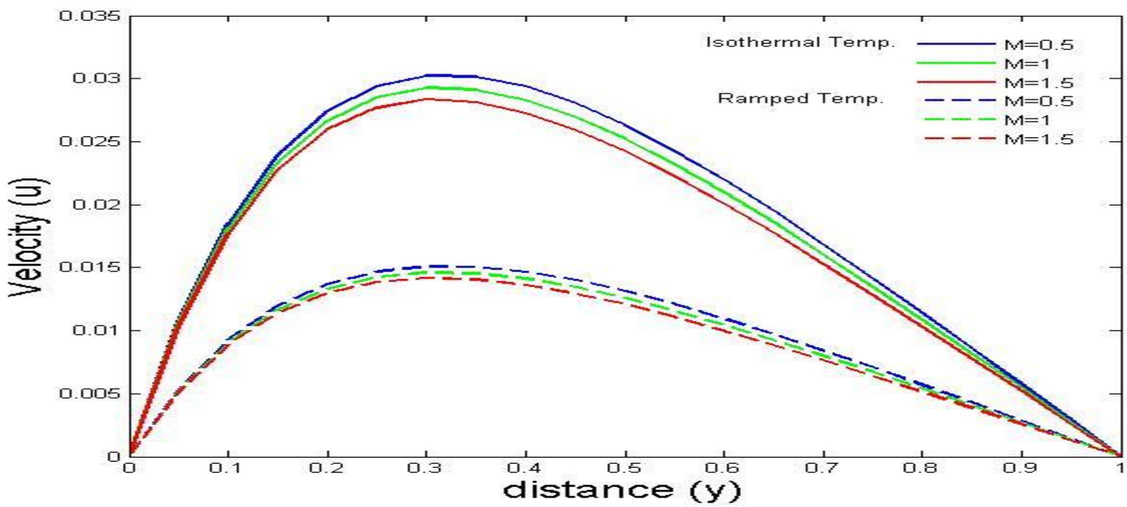

Figure 1: Effect of M on velocity profile

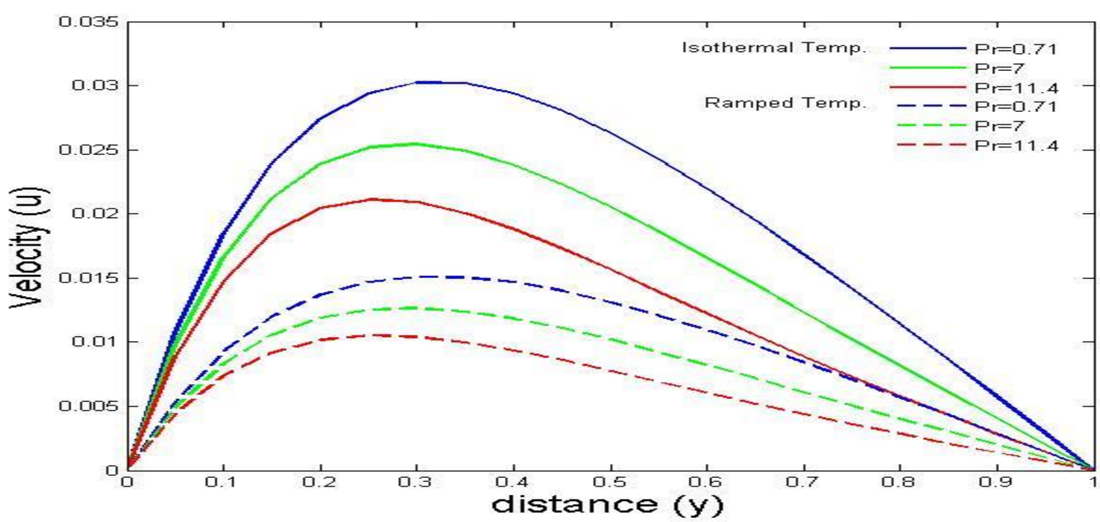

Figure 2: Effect Pr on velocity profile

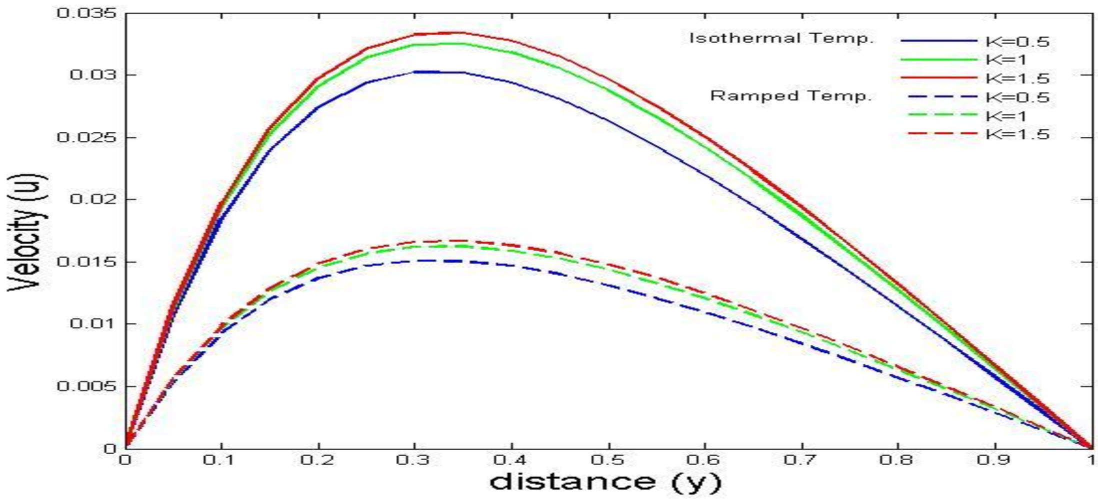

Figure 3: Effect of K on velocity profile

Figure 1 gives the details about the control of magnetic parameter M on velocity for both isothermal and ramped plate. From that figure it is noticed that the velocity begins to reduce at all point of the flow field by increasing the values of magnetic parameter M. This is true since magnetic parameter produce resistive force, which acts opposite direction to the fluid motion. Similarly, Figure 2 gives the details about the control Prandtl number $\Pr$ on fluid velocity for both isothermal and ramped plate. From that figure it is noticed that fluid velocity begins to diminish at all point of the flow field by increasing the values of Prandtl number $\Pr$. While Figure 3 gives the details control about porosity parameter K on fluid velocity for both isothermal and ramped plate and it is also observed that fluid velocity begins to increase at all point of the flow field on increasing the values porosity parameter K.

Figure 4 demonstrates the influence of the ratio of mass transfer parameter N on the fluid velocity for both isothermal and ramped plate. It is observed that the fluid velocity gets enlarged by increasing the values of the ratio of mass transfer parameter N for both isothermal and ramped plate. While Figure 5 demonstrate the influence of Radiation parameter term (R) on the fluid velocity for both isothermal and ramped plate. It is also clearly observed that the fluid velocity gets reduced for both isothermal and ramped plate by increasing the values of Radiation parameter term (R).

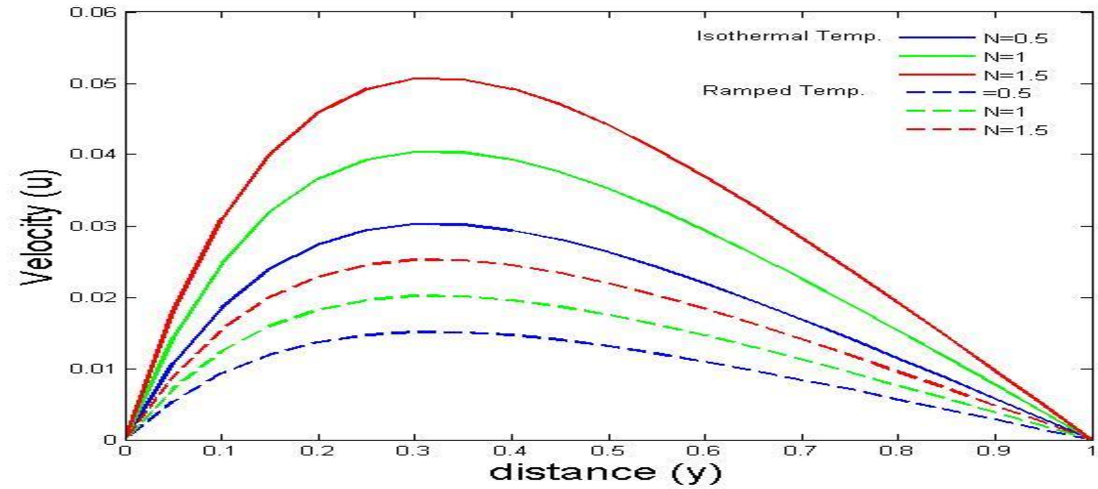

Figure 4: Effect of N on velocity profile

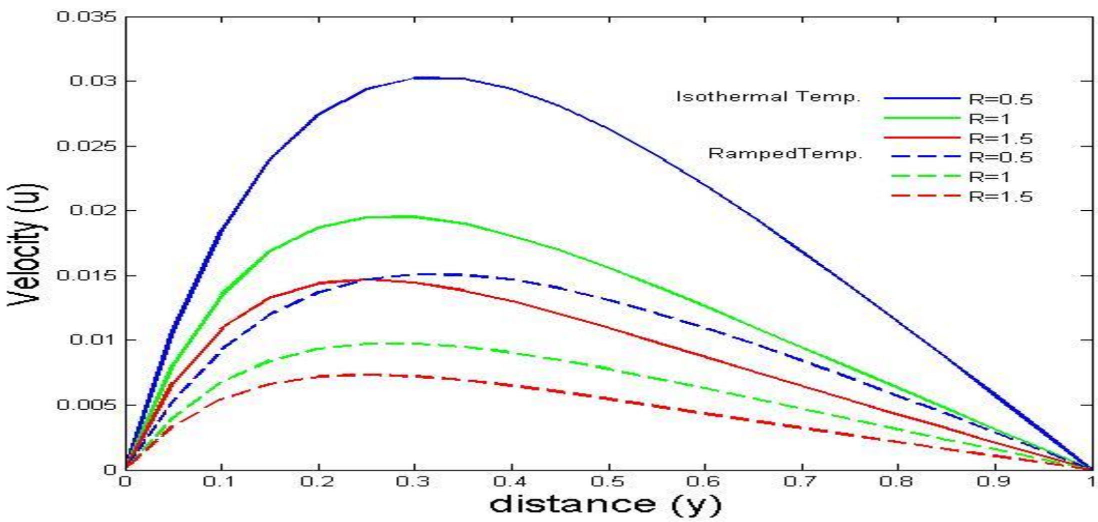

Figure 5: Effect of R on velocity profile

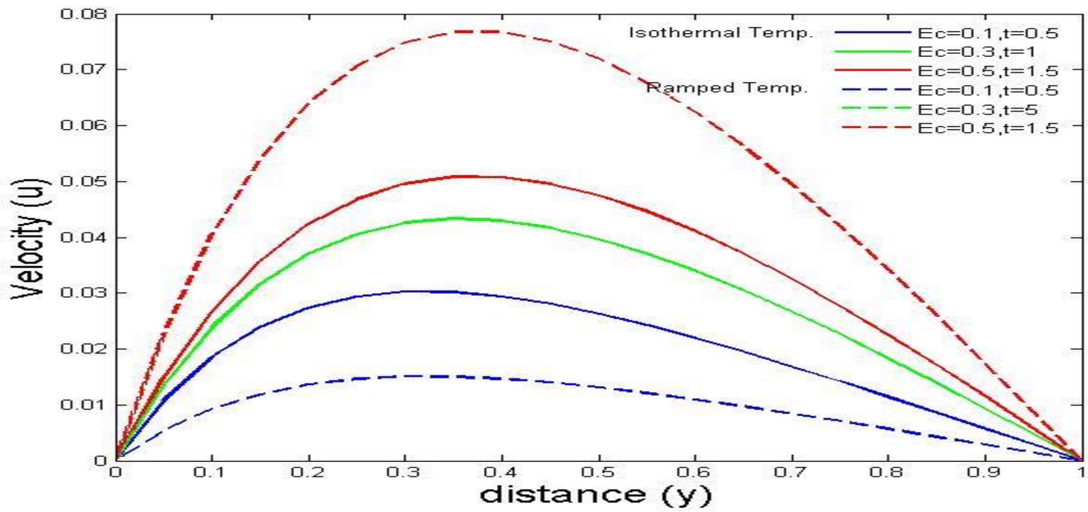

Figure 6: Effect the different values Ec and t on velocity profile

Figure 6 displays the effect of Eckert number Ec and time t parameter on the fluid velocity for both isothermal and ramped plate. It is observed that the velocity get significant enhancement by increasing the values of Ec and time parameter t for both isothermal and ramped plates. There temperature profiles are presented on the following figures:

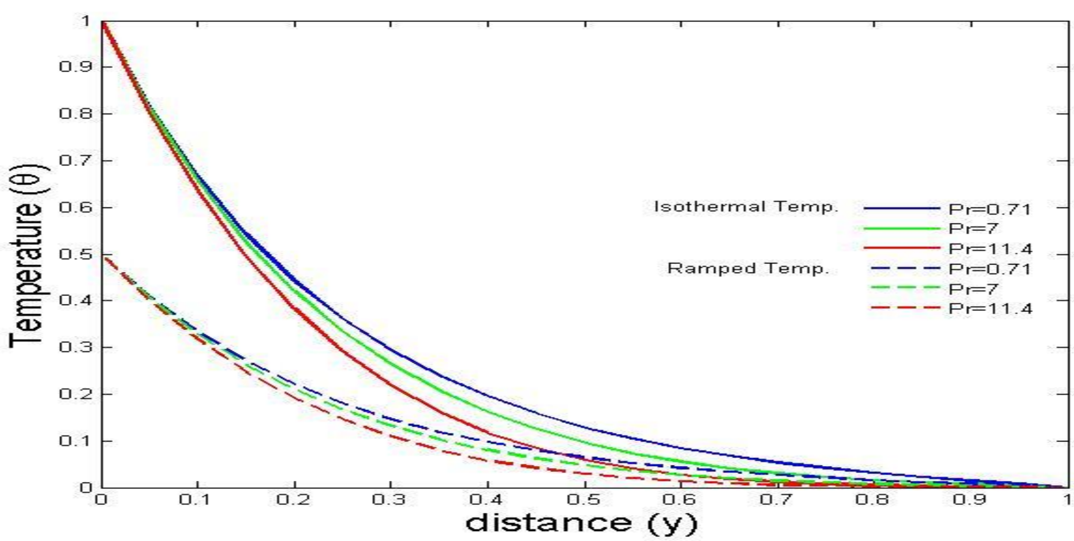

Figure 7: Effect $\Pr$ and on temperature profile

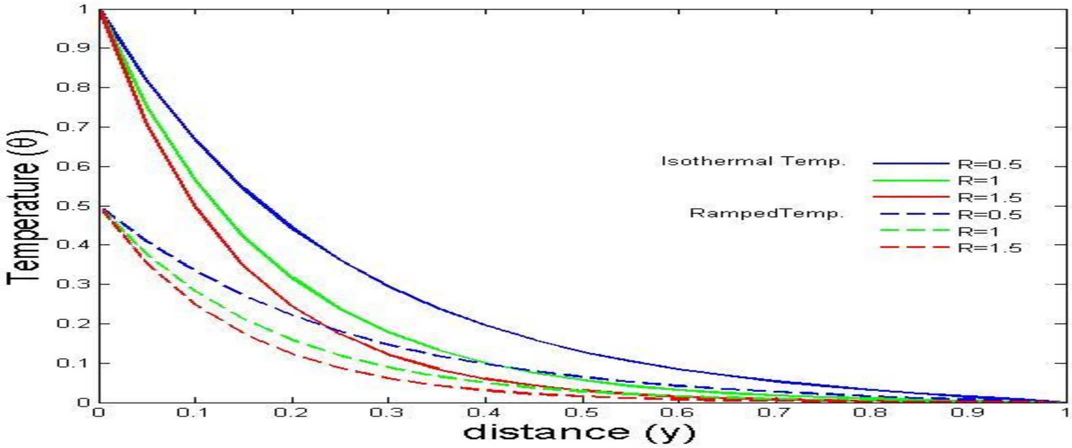

Figure 7: Effect R and on temperature profile

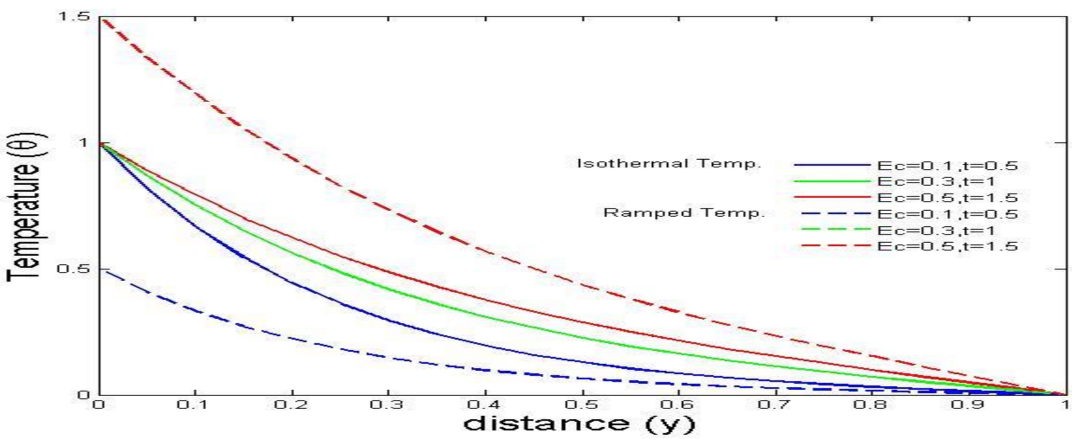

Figure 9: Effect the different values Ec and t on temperature profile

Figure 7 depicts the influence of Prandtl number $\Pr$ on fluid temperature for both isothermal and ramped plate. It is revealed from that figure the fluid temperature diminishes by increasing the values of Prandtl number Pr. Similarly figure 8 depicts the influence of radiation parameter term R on fluid temperature for both isothermal and ramped plate. It is also revealed from the figure that figure the fluid temperature gets reduced by increasing the values of Radiation parameter term R.

Figure 9 displays the effect of Eckert number Ec and time t parameter on the fluid temperature for both isothermal and ramped plate. It is observed that the temperature profile gets enlarged by increasing the values of Eckert number Ec and time parameter t for both isothermal and ramped plate.

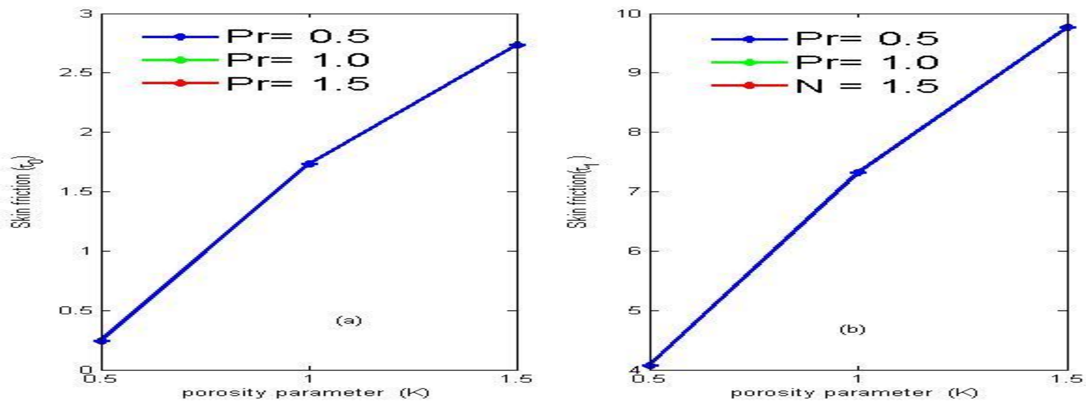

Figure 10(a) &10(b): Effect Pr and K on Skin friction

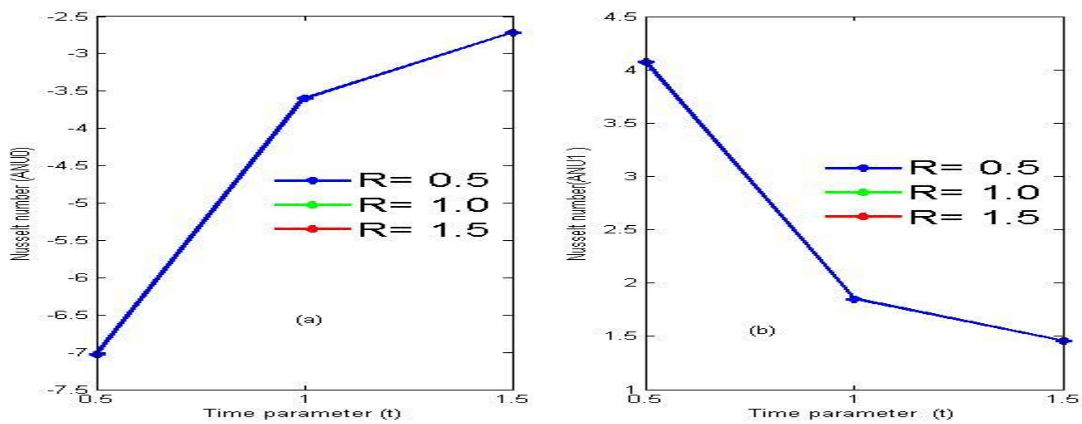

Figure 11(a) &11(b): effect t and R on Nusselt number

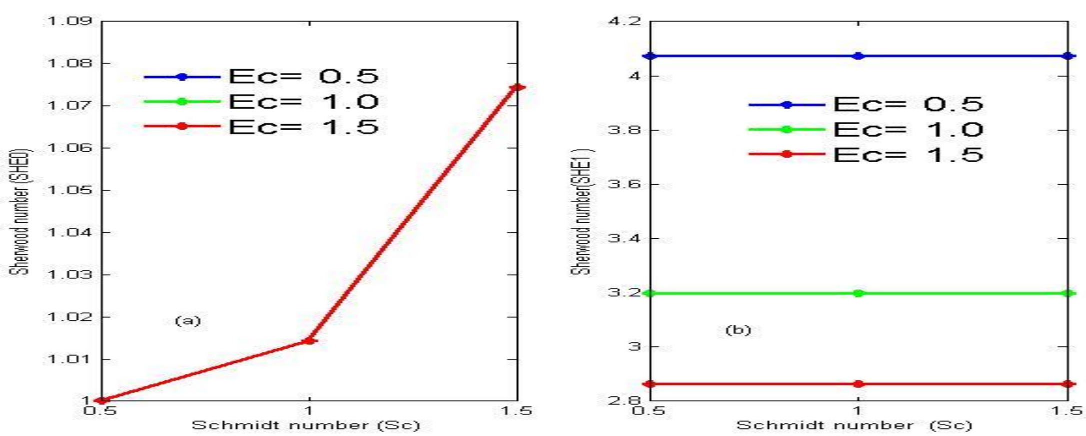

Figure 12(a) &12(b): effect Ec and Sc on Sherwood number

Figure 10(a) and 10(b) displays the effect of Prandtl number Pr and porosity parameter K on the fluid skin friction. It is clearly seen that, increase in Prandtl number has no significant effect on skin friction in both Figure 10(a) and 10(b). While increase in porosity parameter K has boosting effect on skin friction in Figure 10(a) and 10(b). Similarly, Figure 11(a) and 11(b) displays the effect of time parameter and radiation parameter on the Nusselt number. It is clearly observed that in Figure 11(a) increase time parameter t has significant enhancing effect on Nusselt number and increase in radiation parameter has no significant effect on Nusselt number. In Figure 11(b) Nusselt decreases with increasing time parameter t and radiation parameter has no significant effect on Nusselt number. Figure 12(a) and12 (b) displays the effect of Eckert number Ec and Schmidt number Sc on Sherwood number and it is seen that Schmidt number has increasing effect on Sherwood number in Figure 12 (a) and has no significant effect on Sherwood number in Figure 12 (b). Increase Eckert number has no significant effect on Sherwood number in Figure 12(a) and has significant increasing effects on Sherwood number in Figure 12 (b).

5. Conclusion

In this paper, we studied the thermal radiation effects on unsteady heat and mass transfer Couette flow of free convective vertical channels due to ramped and isothermal temperature. From the study, the following conclusions were drawn:

i. Increase of porosity parameter K, ratio of mass transfer parameter N, Eckert number Ec time parameter t enhances the velocity while reverse is the case with the increase of Magnetic parameter M, Radiation parameter tern R and Prandtl number $\Pr$.

ii. Similarly increase of Eckert number Ec and time parameter t enhances the temperature profile and reverse is the case with the increase of Magnetic parameter M, Prandtl number $\Pr$ and Radiation parameter R.

iii. Prandtl number has no effects on skin friction at y = 0 and y = 1, skin friction at y=0 and y=1 gets enlarged with the increase of porosity parameter K.

iv. Increase in radiation parameter R has no effects on Nusselt number at y = 0 and y = 1, but increase in Prandtl enhances the Nusselt number at y = 0 and it diminishes it at y = 1.

v. Schmidt number has boosting effects on Sherwood number at y = 0 and has no effects in Sherwood number at y = 1. While Eckert number has no effects on Sherwood number at y=0 and has significant enlarging effects on Sherwood number at y = 1.

References

1. Adamu, G. C., and Bandari, S. (2018). Buoyancy Effects on MHD Flow of a Nanofluid over a Stretching Sheet with Chemical Reaction. *International Journal of Innovative Research in Science, Engineering and Technology*; 7(11), 2319-8753

2. Alao F. I., Fagbade A. I. & Falodun, B. O. (2016). Effects of Thermal Radiation, Soret and Dufour on an Unsteady Heat and Mass Transfer flow of a Chemically Reacting Fluid past a Semi-Infinite Vertical Plate with Viscous Dissipation. *Journal of the Nigerian Mathematical Society*; 35(2016) 142-158.

2. Animasaun, I. L., Raju, C. S. K. & Sandeep, N. (2016). Unequal Diffusivities Case of Homogeneous Heterogeneous Reactions within Viscoelastic Fluid flow in the presence of Induced Magnetic-field and Nonlinear Thermal Radiation. *Alexandria Engineering Journal* 55, 1595-1606.

3. Bala, I. Y., Kumar, B. J. & Lin, J. (2016). Combined Effects of Thermal Diffusion and Diffusion-Thermo Effects on Transient MHD Natural Convection and Mass Transfer Flow in a Vertical Channel with Thermal Radiation. *International Journal of Scientific Research*; 7, 2354-2373.

4. Bhatti, M. M., Zeeshan, A. & Ellahi, R. (2017). Heat Transfer with Thermal Radiation on MHD Particle fluid Suspension Induced by Metachronal Wave. *Pramana Journal of Physics;* (2017), 39-48. DOI 10.1007/s12043-017-1444-6.

5. Danjuma, Y.I., Haliru, A.A., Ibrahim, M & Hamza, M.M. (2019). Unsteady Heat Transfer to MHD Oscillatory Flow of Jeffrey fluid in a Channel Filled with Porous Material. *International Journal of Scientific and Research Publications,* 9 (7), 2250-3153.

6. Ganesh, K. K., Gireesha B. J., Manjunatha S. & Rudraswamy N. G. (2017). Effect of Nonlinear Thermal Radiation on Double-Diffusive mixed Convection Boundary Layer Flow of Viscoelastic Nanofluid over a Stretching Shee. *International Journal of Mechanical and Materials Engineering;* 10(11), 71-83.

7. Ganesh, K. K., Gireesha B. J., Manjunatha S. & Rudraswamy N. G. (2017). Non Linear Thermal Radiation Effect on Williamson Fluid with Particle-Liquid suspension past a Stretching Surface. *Elservier Journal*; 7(2017), 3196-3202.

8. Nayak, M. K. (2017). MHD 3D Flow and Heat Transfer Analysis of Nano Fluid by Shrinking Surface Inspired by Thermal Radiation and Viscous Dissipation. *International Journal of Mechanical Sciences;* 124-125(2017), 185-193.

9. Prabhakar, R. B. (2016). Mass Transfer Effects on an Unsteady MHD Free Convective Flow of an Incompressible Viscous Dissipative Fluid Past an Infinite Vertical Porous Plate. *International Journal of Applied Mechanics and Engineering*; 21(1), 143-155.

10. Reddy, G. J., Raju, R. S., Rao, J. A. & Gorla, R. S. R. (2017). Unsteady MHD Heat Transfer in Couette Flow of Water at $4^{o}C$ in a Rotating System with Ramped Temperature via Finite Element Method. *International Journal of Applied Mechanics and Engineering;* 22(1), 145-161.

11. Rizwan, U. L. H., Nadeem, S., Hayat, K. Z. & Sher A. N. (2017). Thermal Radiation and Slip Effects on MHD Stagnation point Flow of Nano Fluid over a Stretching Sheet. *Physics E;* 65(2015), 17-23.

12. Shagaiya, D. S. & Daniel, S. K. (2015). Effects of Buoyancy and Thermal Radiation on MHD Flow over a Stretching Porous Sheet using Homotopy Analysis Method. *Alexandria Engineering Journal;* 54, 705-712.

13. Shagaiya, Y. D. & Simon, K. D. (2015). Effects of Buoyancy and Thermal Radiation on MHD Flow over a Stretching Porous Sheet using Homotopy Analysis Method. *Alexandria Engineering Journal;* 54(2015), 705-712.

14. Siva, R. S. & Anjan, K. S. (2016). Finite Element Analysis of Heat and Mass Transfer past an Impulsively Moving Vertical Plate with Ramped Temperature. *Journal of Applied Science and Engineering*; 19(4), 385-392.